Heliyon 5 (2019) e01704

Contents lists available at ScienceDirect

Heliyon

journal homepage: www.heliyon.com

Characterization and thermal conductivity of cellulose based composite xerogels

Sara Rbihi [a,*], Latifa Laallam [a], Mohammed Sajieddine [b], Ahmed Jouaiti [a]

[a] Laboratory of Sustainable Development, Sultan Moulay Slimane University, Beni Mellal, Morocco
[b] Laboratory of Physic and Materials, Sultan Moulay Slimane University, Beni Mellal, Morocco

ARTICLE INFO

Keywords:
Natural product chemistry
Materials science
Materials chemistry

ABSTRACT

This article is based on the elaboration of different combinations of cellulose based xerogel, derived from orange trees, while incorporating mineral and organic fillers such as cellulose nanocrystals (CNC) or olive pomace for a potential use in the field of thermal insulation. The main objective of this study is the creation of an insulating material with developed thermal properties and low thermal conductivity λ by referring to the evaporation technic, while using the technic of the hot plate evolving in a non-stationary regime, which allow developing a simple and inexpensive method with fillers (organic and inorganic) leading to xerogels with higher thermal properties. In addition, a characterization system incorporated in analytical technics such as X-ray diffraction (XRD), scanning electron microscopy (SEM) or optical microscope can highlight the morphological and structural properties, which allow showing a certain alliance between the morphological and geometrical characteristics of the fillers and the control of physical, thermal properties of the xerogels.

1. Introduction

In order to achieve progress in the concept of sustainable development for a long-term agreement with our ecology, ecological and bio-sourced alternatives have taken place to restore a new form of significant yield. Very recently, a new strategy has been developed to generate insulating cellulose xerogel, in order to exploit these energy insulating properties [1].

Cellulose is a renewable material and the most abundant biopolymer on Earth. But also he has very interesting properties such as thermal and chemical stability [1]. Cellulose is a fibrous polysaccharide of β-D-glucopyranosyl units joined by 1, 4-glycosidic bonds [2]. In recent years, cellulose composites have aroused great interest after being physically or chemically modified, especially for the preparation of semiconductor photocatalysts [3].

Although xerogels have low conductivity, they cannot meet the requirements of some new applications, in fact hydrogels are made by condensation of small polymer particles. The liquid is mainly water or alcohol, therefore, the resulting gels are called hydrogels or alkogels. When the water contained in the pores is replaced by supercritical drying, the products are xerogels. When ambient drying conditions are used, xerogels are produced, but these materials are characterized by a large shrinkage during drying and a network of collapsed pores, these limitations have motivated the development of new advanced materials, which is the case of hybrid xerogels, therefore our work is based on the production of new hybrid cellulose materials from orange trees [4]. The properties of xerogels are mainly influenced by the liquid-vapor interface and the physical properties of the solvent (the solvent used in our study is Toluene). in fact the structural and porous properties are determined by the type of the solvent because the drying is carried out by evaporation of the molecules of the solvent [5, 6].

The high surface area and the biodegradable xerogel resource make these materials ideal for various applications such as carbonaceous materials prepared from cellulose acetate [7]. Xerogels also exhibit significant dielectric performance and electrochemical storage abilities related to their structure (density and porosity), as is the case of composites prepared from cellulose nanofibrils (CNF) and reduced graphene oxide (RGO) [8]. In addition, the Cellulose-based biocomposites derived from nature as cellulose xerogels exhibit remarkable mechanical properties which inspire to prepare synthetic biocomposites [9].

Xerogels can be inorganic (silica-based) or organic (cellulose-based). They are generally good super-insulators, but they are relatively fragile. Research has recently been conducted to develop bio-sourced and super-insulating xerogels, thus xerogels based on cellulose or its derivatives

* Corresponding author.
E-mail address: rbihi.sara@gmail.com (S. Rbihi).

https://doi.org/10.1016/j.heliyon.2019.e01704
Received 10 December 2018; Received in revised form 24 March 2019; Accepted 8 May 2019

have been developed. Cellulose xerogels could be a solution to develop biomaterials, especially in the field of thermal insulation while creating both bio-sourced, super-insulating materials, with low environmental impact [1, 4].

The main advantages of using hybrid xerogel as an insulating material by the evaporation method include easy fabrication, reduced cost and an amorphous structure associated with low conductivity, which is the key point of the final composite [10]. But beyond achieving an inexpensive process that responds to the ease of the sol-gel process, we work on recyclable materials and without any undesirable impact on the environment such as cellulose nanocrystals (CNC) or olive pomace. In addition, this study will highlight a certain affiliation between the morphological characteristics of the fillers and the control of the physical and thermal properties of cellulose based xerogels.

2. Materials and methods

2.1. Materials

Sulfuric acid (H_2SO_4) 68%, acetic acid (CH_3COOH) 99.7%, ethanol (C_2H_5OH) 95%, toluene (C_7H_8) 99.8%, Sodium hydroxide (NaOH), Hydrogen Peroxide (H_2O_2) 98%, performic acid (CH_2O_3), peracetic acid ($C_2H_4O_3$) and alginate $(C_6H_8O_6)_n$ and Titanium dioxide (TiO_2) 97% were all supplied by Sigma Aldrich (Germany) and were used without any purification.

2.2. Preparation of cellulose

Cellulose nanofibers with length of more than several (μm) were extracted from orange trees, Beni Mellal, Morocco, which will be the matrix of xerogel, as follows:

- These leaves were harvested at the end of maturity. After being washed thoroughly with water, the leaves are dried in the ambient air. The dry matter was ground in a domestic coffee grinder and sieved on a sieve of homogeneous and low porosity [11].
- Soxhlet extraction: We put 15 g of the product in the cartridge, then in the Soxhlet tank. We fill the flask with a sufficient amount of (ethanol/toluene) solvent (62/38 v/v). Soxhlet extraction takes approximately 72 cycles. The depigmented fibers were then dried at 80 °C for 2 hours in an incubator [12].
- Suspension preparation: The suspension is prepared by 17% of distilled water relative to the weight of the dry pulp, then we put the mixture in a blender. Rotation of the helix at high speed and the resulting increase in temperature causes shearing of the cell wall. The dough is crushed for 40 minutes until a juice is obtained, and then allowed to swell for 8 hours [11, 12].
- Cell swelling: Sodium hydroxide (NaOH) eliminates a good part of the hemicelluloses. The pulp is treated with the solution of sodium hydroxide at 80 °C for 2 hours under magnetic stirrer. The suspension is filtered, washed with water and the treatment is repeated four times [11, 12].
- Bleaching: This treatment allows the elimination of all organic incrustations of the wall (and especially lignin) thanks to the use of performic acid (CH_2O_3) and peracetic acid ($C_2H_4O_3$) in reaction with hydrogen peroxide (H_2O_2). The whole is heated at 80 °C for 3 hours under magnetic stirrer. The suspension is filtered and washed thoroughly with distilled water. The operation is repeated 6 times until the cellulose fibers turn beige weight. At the end, the suspension is filtered and then washed by a solution of sodium hydroxide (NaOH), and then it is heated for 2 hours at a temperature of 90 °C. The pH of the pulp should be in the average of 10 [12, 13].

2.3. Preparation of cellulose nanocrystals (CNC)

The nanocrystals are obtained during a second acid hydrolysis step and with two different types according to the time of hydrolysis (30 min for cellulose nanocrystals with a composition of 50% (CNC/cellulose w/w) (CNC 50%) and 45 min for cellulose nanocrystals with a composition of 25% (CNC/cellulose w/w) (CNC 25%). We will have a reduction in the length for CNC 25% fibers as compared to CNC 50% [14]. 10 g of the beige pulp of cellulose was added to (Distilled water + sulphuric acid) solvent (1:2 v/v). Then the solution is heated to a temperature of 45 °C, the dispersion is homogenized by Ultra-Turrax at 260 rpm for 30 min for CNC 50% as shown in Fig. 4(b), and 45 min for CNC 25%. The suspension is centrifuged for one hour at 6000 rpm in order to remove the largest amount of sulphuric acid, and then dispersed in distilled water and then centrifuged again at 6000 rpm for one hour. This step is repeated several times until the solution is neutralized. Distilled water is used to eliminate possible degradation of the final product [15].

2.4. Xerogel by sol-gel technic

Xerogels prepared by subcritical drying (Evaporative drying) are characterized by: small dimensions, specific geometries (discs and rods), in comparison with aerogels by supercriticall drying, they showed: Less optical transparency and higher density. Therefore, in order to produce xerogel, we need to use the sol-gel process, which is defined as an aggregation that takes place at the nanoscale, this is the crucial step involved in the development of a xerogel. It has a fundamental impact on the solid final structure, it is during the gelation phase, that the solid network is organized and that the final properties of the xerogel resulting from the drying are devellopped [16].

The gels are obtained by chemical reactions that take place in the liquid phase in the presence of precursors (Toluene) to form a solid (colloidal) structure that will give a nanostructured network. Therefore, a suspension based on cellulose is soaked in 1:1 (Distilled water + Toluene) solvent and the gel is expected to be formed (40–75 minutes), then the gel is finally placed in Petri dish by securing the lid halfway. Let the gel dry out for 1–4 days. In this process, the gel is soaked in Toluene, to replace the pore fluid with the aprotic solvent, the liquid is then gently evaporated, causing a partial collapse of the gel [5]. We used for the drying of the xerogel a thermal hood of the laboratory, in fact, the passage of a sufficiently hot and dry current of air inside the hood leads to a drying of the wet sample, we can then have a difference in temperature and partial pressure between the sample and the gas as shown in Fig. 1 [17].

2.5. Preparation of xerogel

2.5.1. Xerogel of cellulose pulp

First, a colloidal suspension is obtained by dispersing 8.5 g of the cellulose pulp $(C_6H_{10}O_5)_n$ in 50 ml of distilled water, then mixed for 10 minutes with Ultra-Turrax, and then for 6 hours with magnetic stirring, after being added to the (Distilled water + Toluene) solvent (1:1 ratio), the gel time is about 45 minutes. Finally, it's poured into Petri dish, and allowed to dry under the fume hood for 72 hours, and then placed in an oven at 50 °C for 48 hours to remove the water traces, as shown in Fig. 4(a) [16, 17, 18, 19, 20, 21, 22].

2.5.2. Xerogel of cellulose pulp and cellulose nanocrystals

The distribution is 50% of pulp and 50% of CNC (CNC 50%) for the first sample, then another one with 75% of pulp and 25% of CNC (CNC 25%). The cellulose pulp and the cellulose nanocrystals are dispersed in distilled water, then the two dispersions are mixed together, the mixture is then subjected to the subcritical drying as already explained. The gel time is about 65 minutes in 1:1 (Distilled water + Toluene) solvent [16, 17, 18, 19, 20, 21, 22].

2.5.3. Xerogel of cellulose pulp and alginate

With the same technic, 50% of cellulose pulp and 50% of alginate $(C_6H_8O_6)_n$ (Alg) powder are dispersed in distilled water [23]. The

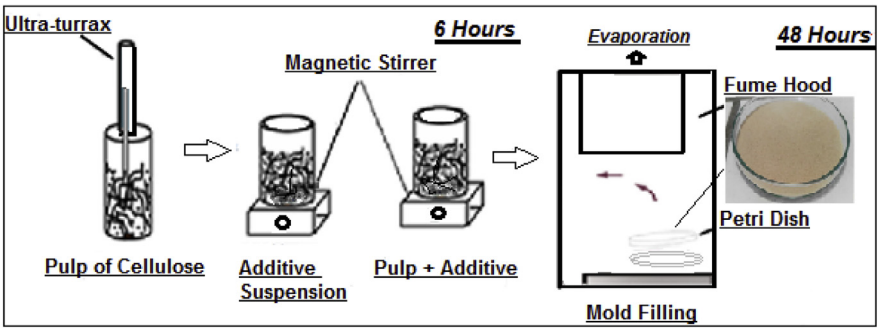

Fig. 1. The process of cellulose based xerogel.

colloidal suspension is homogenised by Ultra-Turrax and magnetic stirring (8 hours), after being added to the (Distilled water + Toluene) solvent, and we wait until the gel is formed (40 minutes). Before, to be placed under the laboratory fume hood for 48 hours [16, 17, 18, 19, 20, 21, 22].

2.5.4. Xerogel of cellulose pulp and titanium dioxide (TiO_2)

75% of cellulose pulp is dispersed with 25% of titanium dioxide (TiO_2) in distilled water, the mixture is homogenised by Ultra-Turrax for 10 minutes and with magnetic stirrer for 6 hours, after being added to the (Distilled water + Toluene) solvent. Then the solution is poured in a Petri dish and kept for 48 hours under laboratory fume hood [16, 17, 18, 19, 20, 21, 22].

2.5.5. Xerogel of cellulose pulp and olive pomace

Olive pomace is the solid by-product obtained from the extraction of olive oil (skin, pulp, and olive kernel). Chemically, it contains cellulose, hemicellulose and lignin. The recycling of by-products solves the environmental problems caused by the olive oil production process [24]. The pomace olive (Oli) is dried in an oven in 60 °C for 4 days. The dry matter was ground in a domestic coffee grinder and sieved on a sieve of homogeneous and low porosity, after, we washed olive pomace with distilled water by a soxhelt to remove the remains of the pulp and oil residues.

With the same technic described above, a Soxhlet extraction with ethanol and toluene mixture is applied, then a cell swelling with sodium hydroxide is applied for one hour in 60 °C under magnetic stirrer, the matter is washed and filtered [11, 12, 13]. Under agitation with Ultra-Turrax, 50% of cellulose pulp with 50% of pomace olive pulp (Oli 50%) are dispersed in distilled water and then homogenised by Ultra-Turrax for 10 minutes and with magnetic stirrer for 6 hours after being added to the (Distilled water + Toluene) solvent (1:1 ratio), the gel time is about 75 minutes. The xerogel is placed under laboratory fume hood for 48 hours. Then we do the same for a second colloidal suspension with 75% of cellulose pulp and 25% of pomace olive pulp (Oli 25%) [16, 17, 18, 19, 20, 21, 22].

2.6. Conductivity meter

The stationary method measures the temperature difference through the Seebeck law, thus the thermal flow of the sample while using the conductivity meter or the hot plate. The thermal conductivity measuring device is based on the production of a thermal gradient according to the thickness of the sample. The first face of the sample is connected to a hot plate which gives the sample an electric power Q, and the other face is linked to a cold cell whose role is to absorb the thermal flow (Fig. 2) [25, 26, 27, 28].

The T-type thermocouple (Cu/Cu–Ni) separated by the sample body measures the difference in temperature ΔT, and the Seebeck coefficient value is (S = 41μv/K) [28], the difference in temperature ΔT follows Eq. (1) [27]:

$$\Delta T = \Delta V/S \tag{1}$$

The thermal conductivity λ is then given by Fourier's law, where Φ is the heat flow, e is the thickness, S is the Seebeck coefficient and ΔV is the voltage difference between the hot and cold sides. we will have the thermal conductivity values in Table 1 [29] using the Fourier equation (Equation 2) [27]:

$$\lambda = {}^{e}/_{\Delta T\, A} \times \Phi \tag{2}$$

Table 1
Thermal conductivity measures.

Samples	ΔV (mV)	ΔT(k)	λ(W.K^{-1}m^{-1})	Density (g/cm^3)
Cellulose	0.70	16.710	0.0339	0.438
TiO_2	1.25	29.840	0.0297	3.149
(CNC 25%)	0.60	14.323	0.0274	0.460
Olive (25%)	0.85	20.291	0.0253	0.584
Alginate (50%)	0.90	21.484	0.0242	0.563
(CNC 50%)	0.95	22.678	0.0232	0.403
Olive (50%)	1.10	26.259	0.0220	0.682

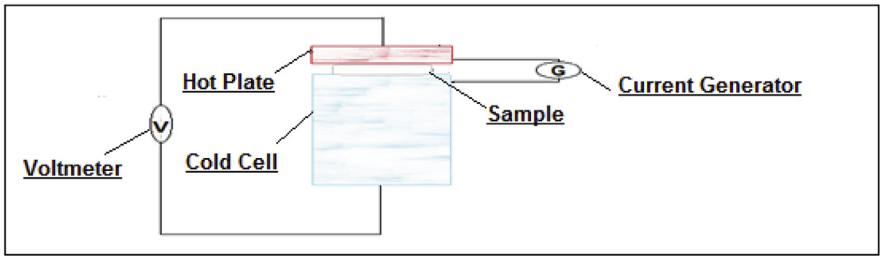

Fig. 2. The thermal conductivity measuring device.

3. Results and discussion

3.1. Conductivity meter results

The stationary method gives the temperature difference through the Seebeck law, then the thermal conductivity by Fourier's law. The values are summarized in Table 1 [30, 31, 32, 33]. Elsewhere, we have studied five types of inclusions with different volume fractions based on the Fourier law and they showed distinct results. From the graph (Fig. 3), we can say that the type of inclusion has the potential to influence the thermal conductivity (the case of cellulose without inclusion 0.0339($W.K^{-1}m^{-1}$) compared to an inclusion of 25% of olive pomace 0.0253($W.K^{-1}m^{-1}$)). For the same volume fraction, we can see differents values of conductivity which reveal that the inclusion volume fraction for the same sample could be a factor influencing the thermal conductivity of the materials.

Thermal conductivity differences were observed between cellulose-based bio-xerogels (Alginate, Olive, CNC) and bio-hybrid xerogels (TiO_2) (Fig. 4). The thermal conductivity of TiO_2 is 29 $mW.K^{-1}m^{-}1$, Alginate is 24 $mW.K^{-1}m^{-1}$ and Olive pomace is 22 $mW.K^{-1}m^{-1}$. There are very few comparative studies between these two types of materials (bio-xerogels and bio-hybrid xerogels) [30, 31, 32, 33]. It has therefore seemed interesting to compare the thermal conductivities of these two types of materials. The differences in behavior were explained from the specificities of each type of nanocharge whether it is cellulosic or mineral. Cellulose nanocrystals are rigid rods of cellulose while mineral fillers are complex porous inorganic substances. hence it can be said that cellulose-based xerogels showed low thermal conductivity as a function of the added charge inclusions.

To visualize cellulose nanocrystals, we used an optical microscope. To characterize the cellulose nanocrystals CNC, we have dispersed a small amount of cellulose nanocrystals in distilled water to obtain an aqueous suspension. Below (Fig. 4), we can observe by optical microscopy, cellulose fibrils from orange fibers.

3.2. Characterization

3.2.1. X-ray diffraction analysis (XRD)

We also used X-ray diffraction analysis (XRD) in order to characterize its crystalline structure and to confirm the presence of crystallinity in the studied material. The identification of the samples were investigated by an X-ray diffractometer (Bruker, D8-Advance) in the reflection mode, using CuKα radiation (λ = 1.5406Å). The diffraction patterns were collected in the 2θ range from 10 to 30°. X-rays are generated by a cathode ray tube. The interaction of the incident rays with the sample produces constructive interference when conditions satisfy Bragg's Law (Equation 3) [34]:

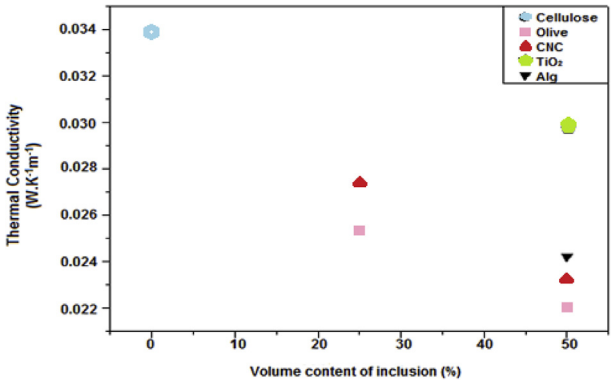

Fig. 3. Comparison of thermal conductivity results.

$$n\lambda = 2d\ \sin(\theta) \quad (3)$$

The diffractogram (Fig. 5(a)) corresponds perfectly to that of cellulose I_β (monoclinic structure) according to the XRD patterns, the diffraction peaks at 2θ around 14.5°, 16.5°, and 24.5°, corresponding to (1–10) (110)and (200). Therefore confirms the nature of the cellulose xerogel with a unit cell of (a = 0.77 nm, b = 0.82 nm, c = 1.03 nm, ϒ = 96°). The figure shows schematically the amorphous and crystalline areas of cellulose [35, 36]. The olive pomace of 25% inclusion xerogel present the same peaks at 14.5 and 24.5 which indicated that the crystalline structure of cellulose xerogel didn't change, but also a part of the crystalline region turned into an amorphous region.

From the graph (Fig. 5(b)), we can see that the diffraction patterns of CNC 25% xerogel were similar to native cellulose xerogel, which refer to the fact that the hydrolysis reaction did not affect the internal crystalline structure of cellulose, but the sharp peaks indicate that the xerogel CNC cellulose is highly crystalline.

The diffraction peak of CNC 50% is more acute and the relative peak intensity is increased, the peak at 14.5 disappeared, and a peak at 15.13 appeared, this indicated that the crystalline structure of cellulose xerogel didn't affect a change. However, we can observe that the diffraction intensity of the new peak had shown a drop, which can be explained by a drop of cellulose crystallinity in xerogel.

3.2.2. The effect of size and crystallinity on thermal conductivity

The size of the crystals τ is given by Scherrer's formula, Where k is a form factor (k = 0.89), λ is the wavelength of x-rays, and β characterizes the width at half-height (full width at half maximum FWHM), i.e. the width of the peak halfway. According to Scherrer's formula (Equation 4) [37]:

$$\tau = k.\lambda/(\beta.\cos(\theta)) \quad (4)$$

We will use the XRD Peak Height Method developed by Segal and we will focus on one very intense peak while comparing it to the others, the values are summarized in Table 2. The crystallinity index is calculated from the ratio of the height of the peak 200 (I_{200}) located at θ = 24.5° and the height of the minimum between the peaks 200 and 101 (I_{AM}) located at approximately θ = 18.5°, as shown in Fig. 5(a) [35, 36]. The crystallinity index is calculated by Eq. (5) [35]:

$$\%\ \text{Crystallinity} = ((I_{200}) - (I_{AM}))/((I_{200})*100 \quad (5)$$

- The smaller the grain size, the greater the phonon scattering, therefore, the thermal conductivity will decrease as shown in Table 2. However, crystallite size depends on the hydrolysis process of H_2SO_4 (synthesis) [14, 15]. Any type of non-uniformity can restrict phonon movement. Grain boundaries are considered defects. Decreasing the grain size means that you increase the grain boundaries, this will reduce the thermal conductivity (Fig. 6).
- The contributions of other crystalline peaks are excluded by keeping only one highest peak (200). The I_{AM} peak will likely be greater than 18.5°, it turned out to be 21° (Fig. 5(a)). By the height method the I_{AM} is underestimated, which leads to an overestimation of the crystallinity. The neglect of the variation of the width of the peak as a function of the size of the crystallites does not make it possible to give an accurate estimate of the crystallinity (Table 2).
- The hydrolysis is intended to intensify the crystalline zone, and the hydrolysis result depends on the time (30 min for CNC 50% and 45 min for CNC 25%) [14, 15]. The difference between CNC 50% and CNC 25% can be explained by the difference in hydrolysis time hence the presence of amorphous areas of cellulose that have not yet disappeared in 50% CNC (30 min). Whereas for CNC 25% (45 min) the dispersion of cellulose nanocrystals has been completed.
- The addition of cellulose nanoparticles in the xerogel decreases their thermal conductivity, it goes from 33.9 ($mW.m^{-1}K^{-1}$) to 23.2

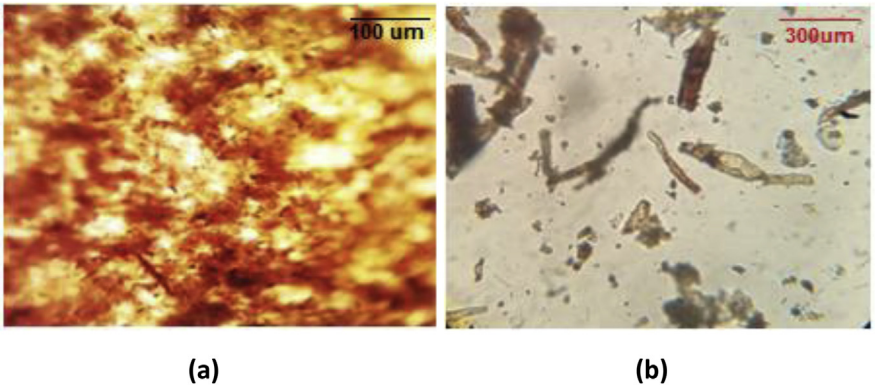

Fig. 4. Optical microscope observation: (a) cellulose pulp, (b) cellulose nanocrystals (CNC 50%) hydrolysis at 30 min.

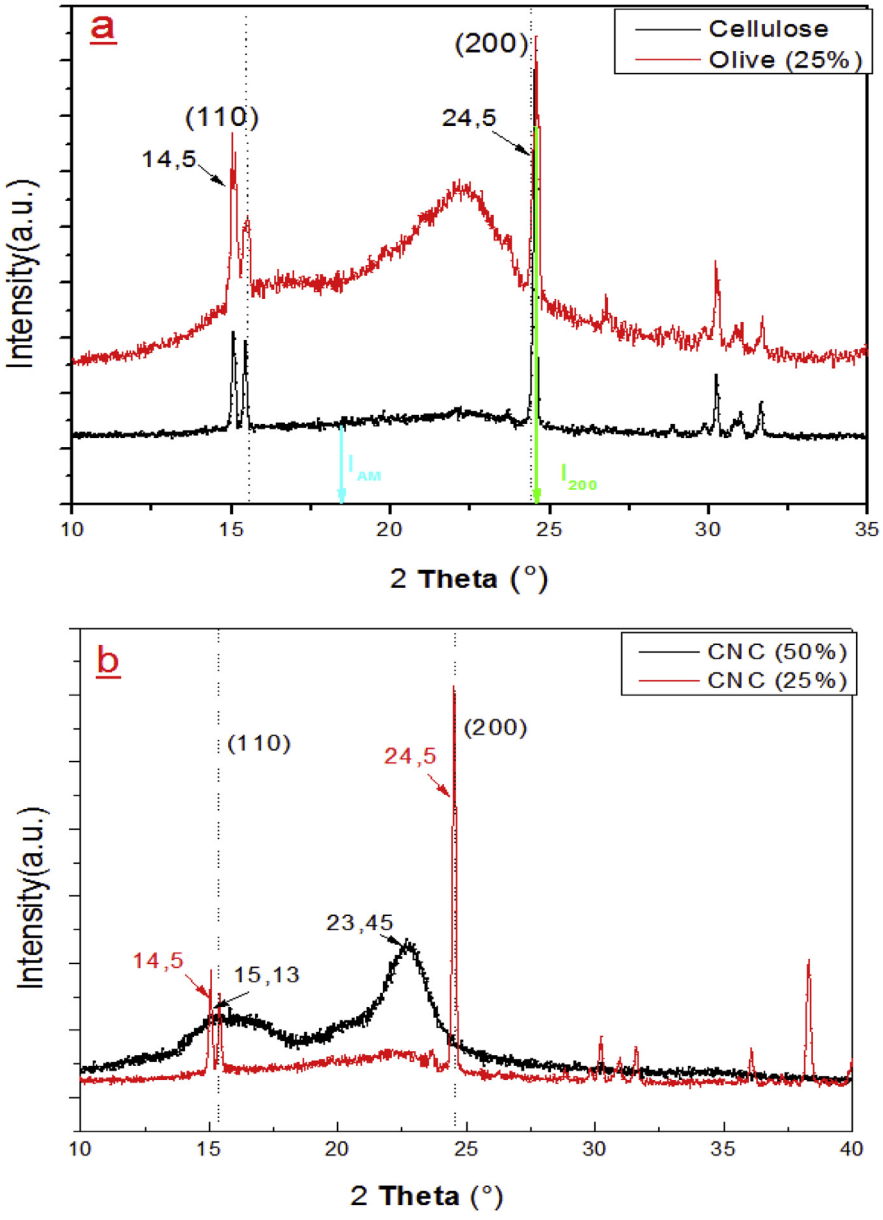

Fig. 5. X-ray diffraction spectrum of: (a) cellulose and olive pomace xerogels, (b) CNC (50%) and CNC (25%) xerogels.

Table 2
Crystallinity measurement values.

Samples	θ (rad)	FHWM (rad)	XRD Crystal size τ (nm)	I_{200}	I_{AM}	Cr (%)	SEM Crystal size τ (nm)	Relative error δ
Cellulose	0.214	0.001	84.68	3365.83	348	89.660	95	0.121
CNC 25%	0.214	0.002	56.45	2796.09	340	87.840	75	0.328
Olive 25%	0.214	0.003	42.34	1775.33	1419	20.071	60	0.416
CNC 50%	0.147	0.020	6.97	32.47	28.3	12.781	12	0.721

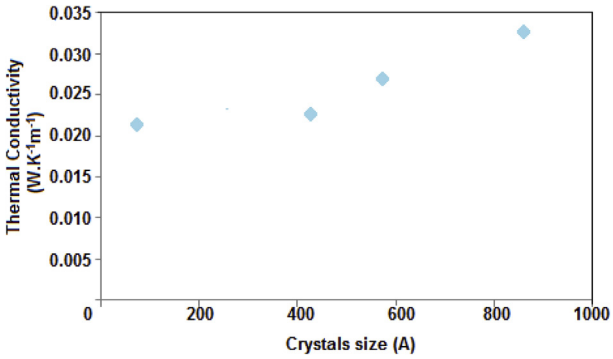

Fig. 6. Thermal conductivity According to Crystals Size.

($mW.m^{-1}K^{-1}$) for the mixture (CNC 50%) [30, 31]. We find that the conductivity decreases as the proportion of CNC is added to the xerogel. This can be correlated with the decrease in crystallite size provided by short fibers (Table 2). The incorporation of more fibers causes a tighter entanglement (the confinement of free air).

- The crystallinity rate of the CNC 25% is 87% against 12% for the CNC 50% seems to have an influence on the conductivity. Nevertheless the crystallinity rate can be influenced by the formation of nano-crystallites and their size distribution which still depend on the parameters of the hydrolysis. The higher the crystallinity, the higher the conductivity (Tables 1 and 2).

3.2.3. *Scanning electron microscopy (SEM)*

The morphology of the samples was investigated by a scanning electron microscope **(JEOL JSM-IT 100)** for cellulose, olive pomace, CNC

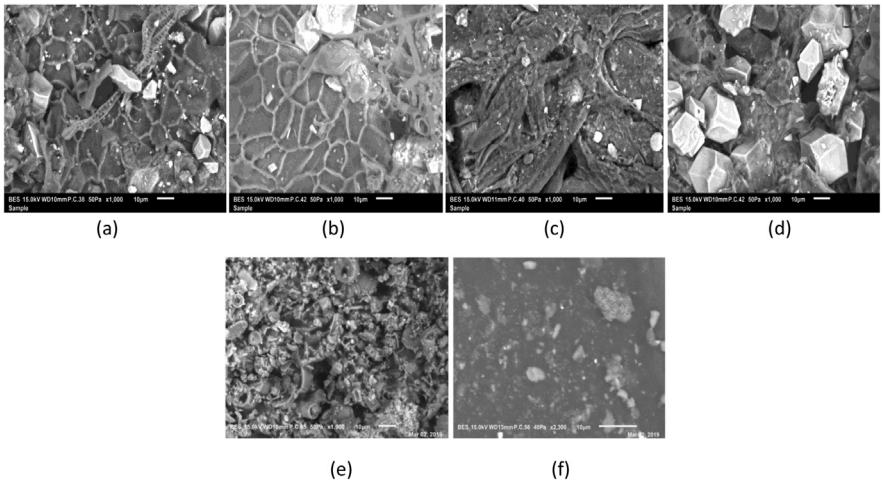

Fig. 7. SEM images of:(a) cellulose xerogel, (b) olive pomace xerogel, (c) CNC 50% xerogel, (d) CNC 25% xerogel, (e) Titanium dioxide xerogel, (f) Alginate xerogel.

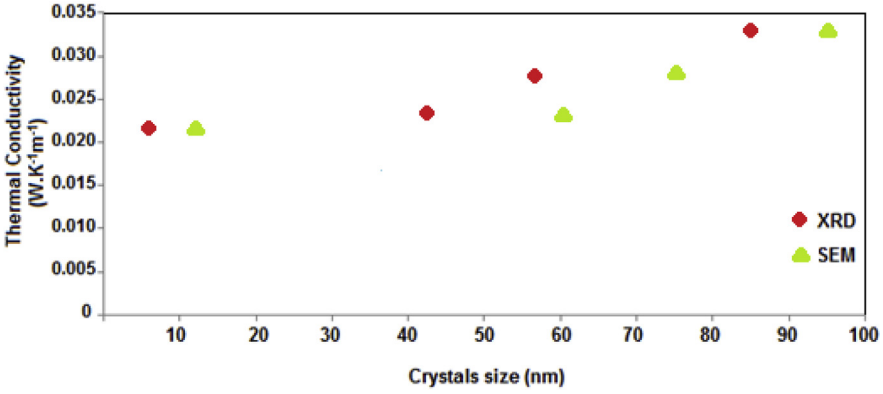

Fig. 8. Thermal conductivity values based on XRD and SEM data.

50%, CNC 25% xerogel, Alginate and TiO_2 xerogel, as shown in Fig. 7. A scanning electron microscope (SEM) scans a focused electron beam over a selected area of the surface of the sample to create an image. The interaction between electrons and the sample produces various signals that can be used to reveal information about the sample including external morphology (texture), chemical composition, and crystalline structure [38].

One of the simplest technics to estimate the average grain size, is the interception technic. A random straight line is drawn through the micrograph. The number of grains cutting the line is counted. The average grain size is obtained by dividing the number of intersections by the actual length of the line. We will use the Image J software (Image J is an open source image processing program) to determine the average size of the nanoparticles in a SEM. It can convert the SEM image into 8 bits, we will get information on each particle. The average size is given by the following Eq. (6) [39]:

$$\text{Average size} = (\text{actual length of line}/\text{number of intersections}) \quad (6)$$

The interception technic was found to give us an overestimate of average grain size (Table 2). The actual grain size will be highly distorted compared to the average calculated from the counted intercepts for geometric reasons (Fig. 8). It is possible that we have not crossed the limits because they are limits of weak angles or small particles decorating them. In this case, conventional average linear interception measures would overestimate grain size because some grains would be combined together and would appear to be larger than they actually are. It can be said that as the size increases, the relative error decreases, which correlates with the interpretations already made. The relative error δ is calculated by Eq. (7) [40]:

$$\delta = (\text{value (SEM)} - \text{value (XRD)})/\text{value (XRD)} \quad (7)$$

In fact, the smaller the size, the more the possibility of combining with others increases, the more the calculated size is overestimated, so that the relative error increases more than the theoretical value of XRD (Table 2).

4. Conclusion

Cellulose-based xerogels has been developed while using cellulose derived from orange as raw materials and by reintegrating the different organic fillers such as cellulose nanocrystals (CNC) and inorganic fillers. Cellulose-based xerogels showed low thermal conductivity as a function of the added filler inclusions, the size of grains and crystallinity.

The thermal conductivities targeted for the materials synthesized in this work are extremely low values around 22 mW m^{-1}. K^{-1}. The thermal conductivities of these materials have been evaluated by the method of the heating plate based on the Fourier law. It remains to be known that these cellulose based xerogels can establish a new notion of sustainable development to limit against pollution, by applying them in different sectors such as construction. It would therefore seem useful to study the biodegradability of these new materials in future works in the production of biodegradable nanocomposites with enhanced properties.

Declarations

Author contribution statement

Sara Rbihi:Conceived and designed the experiments; Performed the experiments; Analyzed and interpreted the data; Wrote the paper.

Latifa Laallam: Analyzed and interpreted the data.

Mohammed Sajieddine: Contributed reagents, materials, analysis tools or data.

Ahmed Jouaiti: Conceived and designed the experiments.

Funding statement

This research did not receive any specific grant from funding agencies in the public, commercial, or not-for-profit sectors.

Competing interest statement

The authors declare no conflict of interest.

Additional information

The thermocouple voltage data associated with this study has been deposited at FLUKE (https://us.flukecal.com/Thermocouple-Table-Voltage-Calculator). The ImageJ data associated with this study has been deposited at ImageJ (https://imagej.nih.gov/ij/).

References

[1] M. Deng, Q. Zhou, A. Du, J. van Kasteren, Y. Wang, Preparation of nanoporous cellulose foams from cellulose-ionic liquid solutions, Mater. Lett. 63 (2009) 1851–1854.
[2] M. Paljevac, M. Primožič, M. Habulin, Z. Novak, Ž. Knez, Hydrolysis of carboxymethyl cellulose catalyzed by cellulase immobilized on silica gels at low and high pressures, J. Supercrit. Fluids 43 (2007) 74–80.
[3] S.A. Zikalala, A.T. Kuvarega, B.B. Mamba, S.D. Mhlanga, E.N. Nxumalo, The effec t of synthetic routes on the physicochemical prope rties and optical response of N-doped titania-oxidized carbon nanotube nanohybrids, Mater. Today Chem. 10 (2018) 1–18.
[4] N. Hüsing, U. Schubert, Aerogels–airy materials: chemistry, structure, and properties, Angew. Chem. Int. Ed. 37 (1998) 22–45.
[5] Nela Buchtova, Tatiana Budtova, Cellulose aero-, cryo- and xerogels: towards understanding of morphology control, Cellulose 23 (4) (2016) 2585–2595. Springer Verlag.
[6] S.R. Venkatasubramanian, R. Manikandan, K. Abirami, V. Karthikeyan, S. Subhalakshmi, Synthesis and characterization of alumina xerogel by epoxide assisted method and subcritical drying, Int. J. Eng. Sci. Invent. ICAFM (2017) 31–35.
[7] J. Štefelová, M. Mucha, T. Zelenka, Cellulose acetate-based carbon xerogels and cryogels, WIT Trans. Eng. Sci. 77 (2013) 65–75.
[8] Y.B. Pottathara, V. Bobnar, M. Finšgar, Y. Grohens, S. Thomas, Cellulose nanofibrils-reduced graphene oxide xerogels and cryogels for dielectric and electrochemical storage applications, Polymer 147 (2018) 260–270.
[9] K. Ganesan, A. Dennstedt, A. Barowski, L. Ratke, Design of aerogels, cryogels and xerogels of cellulose with hierarchical porous structures, Mater. Des. 92 (2016) 345–355.
[10] L. Durães, M. Ochoa, N. Rocha, R. Patrício, N. Duarte, V. Redondo, A. Portugal, Effect of the drying conditions on the microstructure of silica based xerogels and aerogels, J. Nanosci. Nanotechnol. 12 (2012) 6828–6834.
[11] Juan I. Moran, Vera A. Alvarez, Viviana P. Cyras, Analia Vazquez, Extraction of cellulose and preparation of nanocellulose from sisal fibers, Springer Sci. 15 (1) (2007) 150–151.
[12] J. Pérez, J. Muñoz-Dorado, T. de la Rubia, J. Martínez, Biodegradation and biological treatments of cellulose, hemicellulose and lignin: an overview, Int. Microbiol. 5 (2002) 53–63.
[13] S.H. ZeronianM, K. Inglesby, Bleaching of cellulose by hydrogen peroxide, Cellulose 2 (1995) 265–272.
[14] Swati Rao, Enzymatic Hydrolysis of Cellulosic Fiber, Georgia Institute of Technology, 2009, pp. 25–29.
[15] F. Camacho, P. Gonzalez-Tello, E. Jurado, A. Robles, Microcrystalline-cellulose hydrolysis with concentrated sulphuric acid, J. Appl. Chem. Biotechnol. 67 (1996) 350–351.
[16] T. Hobson, K.J. Shea, Bridged bisimide polysilsesquioxane xerogels: new hybrid organic-inorganic materials stephen, Chem. Mater. 9 (1997) 616–623.
[17] G. Pajonk, Drying methods preserving the textural properties of gels, Rev. Phys. Appl. 24 (1989) 13–22.
[18] F. Fischer, A. Rigacci, R. Pirard, S. Berthon-Fabry, P. Achard, Cellulose-based aerogels, Polymer 47 (2006) 7636–7645.
[19] M. Guglielmi, G. Kickelbick, Sol-Gel Nanocomposites, Springer, 2014, pp. 1–19.
[20] Kyung Moon Choi, Kenneth J. Shea, Preparation of nano-sized chromium clusters and intimate mixtures of chromium/CdS phases in a porous hybrid xerogel by an internal doping method, J. Am. Chem. SOC. 116 (1994) 9052–9060.
[21] B.A. Rozenberg, R. Tenne, Polymer-assisted fabrication of nanoparticles and nanocomposites, Prog. Polym. Sci. 33 (2008) 40–112.
[22] A.C. Balazs, T. Emrick, T. P Russell, Nanoparticle polymer composites: where two small worlds meet, Science 314 (2006) 1107–1110.
[23] G. Orive, S. Ponce, R.M. Hernández, A.R. Gascón, M. Igartua, J.L. Pedraz, Biocompatibility of microcapsules for cell immobilization elaborated with different type of alginates, Biomaterials 23 (2002) 3825–3831.
[24] José A. de la Casa, Eulogio Castro, Recycling of washed olive pomace ash for fired clay brick manufacturing, Constr. Build. Mater. 61 (30) (june 2014) 320–326.

[25] Dongliang Zhao, Xin Qian, Xiaokun Gu, Saad Ayub Jajja, Ronggui Yang, Measurement Techniques for Thermal Conductivity and Interfacial Thermal Conductance of Bulk and Thin Film Materials, J. Electron. Packag 138 (4) (December 2016).
[26] M. Necati Ozisik, Heat Conduction, second ed., 1993, pp. 1–32. Department of Mechanical and Aerospace Engineering, North Carolina State, University Raleigh, North Carolina, A Wiley-Interscience Publication JOHN WILEY & SONS, INC.
[27] H. Jung Kim, J.R. Skuza, Y. Park, Glen C. King, Sang. H. Choi, A. Nagavalli, System to Measure Thermal Conductivity and Seebeck Coefficient for Thermoelectrics, National Aeronautics and Space Administration (NASA) Langley Research Center Hampton, Virginia, 23681-2199, December 2012, pp. 1–8.
[28] A.W. Van Herwaarden, P.M. Sarro, Thermal sensorsbased on the seebeckeffect, Sensor. Actuator. 10 (1986) 321–346.
[29] J. Martin, T. Tritt, C. Uher, High temperature Seebeck coefficient metrology, J. Appl. Phys. 108 (2010), 121-101.
[30] Georg Pour, Christian Beauger, Rigacci Arnaud, Tatiana Budtova, Xerocellulose: lightweight, porous and hydrophobic cellulose prepared via ambient drying, J. Mater. Sci. 50 (2015) 4526–4535.
[31] A. Rigacci, J.C. Marechal, M. Repoux, M. Moreno, P. Achard, Preparation of polyurethane-based aerogels and xerogels for thermal superinsulation, J. Non Cryst. Solids 350 (2004) 372–378.
[32] Lin-Yu Long, Yun-Xuan Weng, Yu-Zhong Wang, Cellulose Aerogels: Synthesis, Applications, and Prospects Polymers, vol. 10, 2018, pp. 3–28.
[33] A. Bisson, A. Rigacci, D. Lecomte, P. Achard, Effective thermal conductivity of divided silica xerogel beds, J. Non Cryst. Solids 350 (2004) 379–384.
[34] V. Drits, J. Środoń, D.D. Eberl, XRD measurement of mean crystallite thickness of Illite and Illite/Smectite: reappraisal of the kubler index and the scherrer equation, Clay Clay Miner. 45 (1997) 461–475.
[35] M. Ya. Ioelovich, G.P. Veveris, Determination of cellulose crystallinity by X-ray diffraction method, J. Wood Chem. 5 (1987) 72–80.
[36] A. Isogai, M. Usuda, Crystallinity indexes of cellulosic materials, Seni Gakkai Shi 46 (8) (1990) 324–326.
[37] Monshi Ahmad, Mohammad Reza Foroughi, Mohammad Reza Monshi, Modified scherrer equation to estimate more accurately nano-crystallite size using XRD, World J. Nano Sci. Eng. 2 (2012) 154–160.
[38] Demilecamps Arnaud, Synthesis and Characterization of Polysaccharide-Silica Composite Aerogels for thermal Superinsulation, Materials, Ecole Nationale Supérieure des Mines de Paris, 2015.
[39] A. Ali Al-Bakoosh, J. Idris, Impact of rare earth elements Ce and Pr addition on grain refinement of AA5083 alloy, J. Chem. Technol. Metall. 53 (5) (2018) 916–923.
[40] K. Chhetri, Computation of errors and their analysis on physics experiments, Himal. Phys. 3 (2013) 78–86.